SUPPLEMENTAL MATERIAL

Supplemental Methods

Study Populations.

AM patients were identified from a daily review of inpatient ward lists and CMR patient lists. AM was diagnosed on the basis of clinical and CMR findings according to the most recent European Society of Cardiology (ESC) guidelines. [2] In short, all AM patients (n=34) presented acutely with elevated serum cardiac troponin as evidence of acute myocardial injury, CMR tissue characterization was suggestive of myocarditis [70-71], and the absence of coronary disease (Table S2) was demonstrated either by coronary angiography or CMR when the admitting team thought an acute myocardial infarct highly unlikely.[72-74]

DCM was defined by LV systolic impairment and dilatation in the absence of abnormal pressure or volume overload and in the absence of known coronary artery disease sufficient to explain the LV dilatation and systolic impairment.[76]

In patients fulfilling these criteria, idiopathic DCM (iDCM) was defined by the absence, at recruitment, of a family history and/or identified genetic cause of DCM. All iDCM patients were prospectively identified from outpatient clinic or CMR lists.

Acute STEMI patients were all recruited within 2 days of a first-ever presentation with acute chest pain, ST-segment elevation, elevated serum cardiac troponin, and angiographically confirmed occlusion of a main epicardial coronary artery.

Sjögren' s syndrome (SS) patients were diagnosed according to the 2016 American College of Rheumatology (ACR)/European League Against Rheumatism (EULAR) criteria. All patients showed circulating anti-Ro/SSA and/or anti-La/SSB autoantibodies and/or inflammatory infiltration within labial salivary gland biopsies, with severity evaluated based on the focus score index (number of infiltrates containing >50 lymphocytes per 4 mm2 tissue). Disease activity was evaluated with the EULAR SS disease activity index (ESSDAI). Demographics of the SS patients enrolled are listed in Table S3.

Patients with ischemic heart failure (IHF) required a history of myocardial infarction (MI), coronary revascularization, or CMR features consistent with prior MI. Patients had to have current or previous evidence of left ventricular (LV) dysfunction. Previous cardiac resynchronization therapy or ICD implant was taken as sufficient evidence for LV dysfunction if no imaging was available.

Patients with mutations pathogenic for either familial dilated cardiomyopathy and/or arrhythmogenic cardiomyopathy (fHMD) were studied as part of collaborative research targeting those conditions and are included as a second control group (Tables S2, S4). This cohort includes variable clinical phenotypes (some but not all had LV dysfunction) and several had implanted cardiac devices.

Healthy controls had no recent (within 4 weeks) symptoms of a viral illness and did not have a prior cardiac history or a family history for any cardiomyopathy.

Recruitment of at least 20 patients in AM, iDCM and STEMI groups allowed for subject dropout and reclassification. Power calculations were performed in G*Power (G*Power, University of Kiel, Kiel, Germany).

Sample Processing (human samples)

All subjects provided venous blood samples in potassium-ethylenediaminetetraacetic acid (K-EDTA) anticoagulant. The samples were stored at 4oC until processing within 24 hours of collection. After initial centrifugation plasma was aliquoted and stored at -80^{o}C. Peripheral blood mononuclear cells (PBMCs) were isolated from the remaining sample after Ficoll density gradient centrifugation. The PBMCs were washed twice with PBS and then stored at -80^{o}C in freezing medium (90% fetal calf serum (FCS), 10% dimethylsulfoxide (DMSO)) until further analysis. All human samples used in the study were previously frozen, however previous comparison did not show significant differences in the representation of T-cell populations compared to fresh samples (not shown).

Flow Cytometry (human samples)

T-cells were gently thawed by pipetting into RPMI and washed twice in PBS before staining for surface markers with commercially available fluorochrome-conjugated antibodies. Following surface staining, cells were fixed and permeabilized according to manufacturer's instructions (Thermo Fisher, Cat. 00-5523-00) for intracellular staining for FoxP3 and cMet. In human samples, separate intracellular cytokine staining was performed after a 4-hour phorbol myristate acetate (PMA) and ionomycin stimulation with Brefeldin A (Biolegend, Cat. 423304) following surface marker staining, fixation and permeabilization according to manufacturer's instructions (BD Biosciences, Cat. 554714).

Samples were acquired on a LSRII Fortessa flow cytometer (BD Biosciences, San Jose, California, USA) equipped with 405, 488, 560 and 641nm lasers, BD cytometer setup and tracking beads were routinely used to calibrate the cytometer. Single stain and fluorescence minus one control were acquired for compensation and precise gating, respectively. Compensation was automatically calculated, and samples analyzed on dedicated software (FlowJo version 10, FlowJo LLC, Oregon, USA).

Cytokine and chemokine measurement (human cells)

A flow cytometry-based multiplex plasma analysis was performed for pre-determined cytokines and interleukins as stated in Supplemental data Table S1. Standards and patient plasma samples were processed in duplicates as stated by the manufacturer of the multiplex kit (Biolegend, 740930) and acquired on a LSRII Fortessa flow cytometer (BD Biosciences, San Jose, CA, USA). Flow cytometry results were analyzed on automated software provided by the kit manufacturer (LEGENDplex, version 7.0, Biolegend, San Diego, California USA). Using the standard samples, the software automatically constructed standard curves with a 5-parameter curve fitting algorithm – patient sample concentrations were then calculated from the standard curves.

Cardiac Peptide and Tetanus Toxoid Proliferation Assay

PBMCs were thawed and washed as previously described, live cells counted via Trypan blue exclusion and then stained with a proliferation marker (Tag-it-violet) as per the manufacturer's instructions (Biolegend, 425101). Following this, $1x10^5$ PBMCs were plated in 96-well V-bottom plates in culture media (IMDM supplemented with pen-strep and heat-inactivated human AB) and co-cultured with PBS (negative control) or a non-specific antigen Tetanus Toxoid (Sigma, 582231) or individual cardiac antigens reputed to be important antigens in acute myocarditis isolated from human hearts; myosin heavy chain (Sigma, M5074), myosin light chain (Sigma, M4824), Troponin T (Sigma, T0175), Troponin I (Sigma, T9924) and myoglobin (Sigma, M6036).

The cells were incubated in a 37°C incubator for 7 days. Cells were then washed and stained to allow identification of live $CD3^+$ T-cells along with staining to differentiate c-Met^+ from c-Met^- cells.

Myocarditis and iDCM tissue analysis

A total of 10 formaldehyde-fixed and paraffin-embedded samples of human myocardial tissues, including 5 cases with lymphocytic myocarditis and 5 cases with DCM, who either died suddenly or underwent cardiac transplantation, have been examined. 5-µm-thick sections were stained with hematoxylin–eosin and or immunohistochemical studies to analyze the distribution and the

lineage of inflammatory populations in the tissues. Myocarditis was diagnosed in the setting of myocyte necrosis, interstitial edema, and inflammatory cell infiltrates according to established criteria (2). Inflammatory dilated cardiomyopathy was diagnosed in presence of myocytes enlargement with perinuclear halo, replacement fibrosis and inflammatory foci (2013 Nov;18(6):673-81). All human tissues were obtained for diagnostic purposes and anonymized.

For immunofluorescence staining, sections were deparaffinized and dehydrated in Xylol at 100% for 15 minutes (Sigma, 1330-20-7) and further dehydrated in ethanol steps, 100%-95%-80% for 2 minutes (Sigma, 51976) each. They were then placed in deionized water for 2 minutes. Samples were preheated in a citrate buffer then incubated in Goat serum buffer (Sigma, G9023) for 45 minutes, then washed in PBS. Slides were subsequently incubated with the relevant primary antibody, CD3 (Origene, UM500048, 1:200 dilution) and cMet (Abcam, ab51067 1:200 dilution) at 4^{o}C overnight. After washing with phosphate-buffered saline, the sections were incubated with Cy5 (Thermofisher, M35011) -conjugated goat anti-mouse antibody for CD3, and with FITC (Thermofisher, F-2765) -conjugated goat anti-rabbit antibody for cMet. The nuclei of the sections were stained with 4,6-diamidino-2-phenylindole (Thermofisher, D1306). Slides were then mounted and imaged using a Nikon-a1r confocal microscope. Quantification of infiltrating T-cells in each patient was done by averaging the number of $CD3^{+}$ $cMet^{+}$ and $CD3^{+}$ $cMet^{-}$ in 4 20X field from the same patient samples using ImageJwin64 V 1.52p. Mean T-cell infiltration was calculated on the averages from 5 different patients.

Confocal analysis of infiltrating T-cells in human cardiac tissue

Formalin-fixed, paraffin-embedded human heart sections were used for the immunofluorescence staining. Sections were deparaffinized and dehydrated in Xylol at 100% for 15 minutes (Sigma, 1330-20-7) and further dehydrated in ethanol steps, 100%-95%-80% for 2 minutes (Sigma, 51976) each time. They were then placed in deionized water for 2 minutes. Samples were preheated in a citrate buffer then incubated in Goat serum buffer (Sigma, G9023) for 45 minutes, then washed in PBS. Slides were subsequently incubated with the relevant primary antibody, CD3 (Origene, UM500048, 1:200 dilution), or CD4 (Origene, UMAB64, 1:100 dilution), or CD8 (Daco, M7103, 1:100 dilution), and cMet (Abcam, ab51067 1:200 dilution) at 4^{o}C overnight. After washing with phosphate-buffered saline, the sections were incubated with Cy5 -conjugated goat anti-mouse antibody for CD3 (Thermofisher, M35011), and with FITC-conjugated goat anti-rabbit antibody for cMet (Thermofisher, F-2765) with AF555–conjugated goat anti-mouse igG2 for CD4 (Thermofisher, A-21422) and AF647–conjugated goat anti-mouse igG1 for CD8 (Thermofisher, A-21240). The nuclei of the sections were stained with 4,6-diamidino-2-phenylindole

(Thermofisher, D1306). Slides were then imaged using a Nikon-a1r confocal microscope. Quantification was done via ImageJwin64 V 1.52p software.
software.

Quantitative real-time polymerase-chain reaction (qRT-PCR). Cells were harvested and stored in RNA-later (Qiagen, Crawley, UK) at –80°C until processing. RNA was purified using Trizol reagent according to the manufacturer's instructions (Life Technologies) and assessed for quality and quantity using absorption measurements. Reverse transcription was performed according to the manufacturer's instruction (Applied Biosystems). Gene expression analysis was done using SYBR Green Supermix (Biorad) in CFX connect light cycler (Biorad), according to the manufacturer's instructions. Expression was calculated using the ΔΔct method [8] and normalized to a housekeeper gene (GAPDH). Primers for qPCR were designed with the help of online tools (Primer 3Plus) using at least one exon junction-binding site per primer pair. The sequences of the qPCR Primers are as follows:

OR1L3 - (5' ATCCACTCTGATCCTCGACTTC 3' and 5' CATAGCCGCCAGGAGATAACTA 3'), *OR4P4* - (5' AGCTCTTGCCACTTGTAGTTC 3' and 5' CCTCATGGCGTTCTTCATCTCT 3'), *CD22* - (5' CACCTCAATGACAGTGGTCAG 3' and 5' TGGATCGGATACCCATAGCAG 3'), *IL1B* - (5' AGCTACGAATCTCCGACCAC 3' and 5' CGTTATCCCATGTGTCGAAGAA 3'), *IFNg* - (5' TCGGTAACTGACTTGAATGTCCA 3' and 5' TCGCTTCCCTGTTTTAGCTGC 3'), *Tbox21* - (5' TTGAGGTGAACGACGGAGAG 3' and 5' CCAAGGAATTGACAGTTGGGT 3'), *RORgT* - (5' AAGAAGCCCTTGCACCCCTCACA 3' and 5' AAGAAGCCCTTGCACCCCTCACA 3'), *IL22* - (5' GCTTGACAAGTCCAACTTCCA 3' and 5' GCTCACTCATACTGACTCCGT 3'), *Gata3* - (5' GCCCCTCATTAAGCCCAAG 3' and 5' TTGTGGTGGTCTGACAGTTCG 3'), *AHR* - (5' CAAATCCTTCCAAGCGGCATA 3' and 5' CGCTGAGCCTAAGAACTGAAAG 3'), *GAPDH* - (5' GGCTCATGACCACAGTCCA 3' and 5' CACATTGGGGGTAGGAACAC 3')

The thermal cycling profile for amplification was 95°C for 10 min, followed by 40 cycles of 95°C for 15 s and 54°C for 1 min. Amplification was 95°C for 10 min, followed by 40 cycles of 95°C for 15 s and 60°C for 1 min. To ensure the amplification specificity, the melting curve program was set as follows: 95°C for 15 s, 60°C for 1 min, and 95°C for 15 s, right after the PCR cycles.
The qPCR data were analyzed using the delta CT method by taking the CT values of the genes of interest from the house keeping gene following by normalization to the control sample.

The microarray studies used 50ng of RNA input. First strand cDNA was prepared, cRNA synthesised and amplified and second strand cDNA synthesised, fragmented and labelled using the GeneChip WT Plus kit (ThermoFisher, UK; cat no. 902280). Each Clariom D Gene Chip was loaded with 5.2ug ssDNA as per manufacturers protocol. The microarrays were hybridised for 16 hours at 45^{o}C with rotation at 60rpm as per manufacturers protocol. After hybridisation the microarrays were washed and stained using the GeneChip Hybridization, Wash, and Stain Kit (ThermoFisher, UK; cat no. 900720) before scanning with the GeneChip Scanner 3000 (ThermoFisher, UK).

Affymetrix Human Clariom D arrays were normalised via the Robust Multiarray Average (RMA) approach using limma v3.44.3 in R v 4.0.3. Probe IDs were mapped to HGNC symbols using the clariomdhumantranscriptcluster.db v8.7.0 annotation package. Differential expression analysis was performed using limma and using 'Donor' as a covariate to adjust for donor-specific effects. P values were adjusted via the Benjamini-Hochberg method. Principal component analysis (PCA) was performed using PCAtools v2.5.13. Outlier samples (totalling 4) were filtered out after inspection via a PCA bi-plot of PC1 vs PC2. Heatmaps and clustering were performed using ComplexHeatmap v2.4.3. Genes were selected for clustering by taking a union of differentially expressed genes from the CD4 and CD8 comparisons for cMet^{+} versus cMet- based on cut-offs: absolute $\log_2$ fold-change < 0.5 and p-value < 0.05. Volcano plots were generated using EnhancedVolcano v1.11.3. Gene enrichment analysis was performed using differentially expressed genes using KEGG profile v1.30.0 and top GO v2.40.0.

In silico analysis of scRNA data

We accessed the GEO GSE145154 dataset (https://www.ncbi.nlm.nih.gov/geo/query/acc.cgi?acc=GSE145154) and reanalyzed the scRNA count reads, as previously described. [30] In brief, we used the Seurat software (v4.0.6) to integrate all batches, after excluding cells that had fewer than 800 UMI or over 8000 UMI and cells that had more than 10% mitochondrial UMI counts. Prior to integration we: 1) performed log-normalization and identified 2000 variable features per donor, 2) we identified anchors among batches while specifying the normal datasets as the reference. We scaled the integrated data and performed Principal Component Analysis (PCA) and performed cell clustering as described by the authors. [30] Cell clusters were manually annotated, and we performed a second round of clustering on the T-cell populations, as previously described. [30] We manually annotated the T-cell clusters as A (possibly cMet+) and B (rest of the T-cell clusters). We performed differential gene expression

analysis between the two T-cell clusters using the MAST test implemented in the Seurat software (logfc.threshold=0.25, min.pct to 0.1). We considered differentially expressed genes at $p<0.01$.

Animals

All animal protocols used in this study were approved by the Animal Use and Care Committee of Queen Mary University of London (QMUL), following the Home Office Guidance (Scientific Procedure Act 1986), and the Guide for the Care and Use of Laboratory Animals of the National Research Council.

Five-week-old male Balb/cAnN male mice purchased from Charles River Laboratories UK Ltd. (Kent, UK). Animals were allowed to acclimatize to laboratory conditions for one week before any experimental procedure started.

Non obese diabetic (NOD) mice were bred in house and blood glucose levels were monitored daily. Mice displaying fasted blood glucose levels higher than 150mg/dl on 3 consecutive days were considered pre-diabetic, and mice with fasted blood glucose levels around 250 mg/dl for 3 consecutive days were considered diabetic.

All mice had free access to standard diet, water ad libitum, and were housed in a temperature-controlled room (25 ± 2 °C) which had a 12-hour light/dark cycle and individually ventilated cages.

Experimental Autoimmune Myocarditis (EAM)

BALB/cAnN 5-week-old male mice received two subcutaneous injections of cardiac myosin heavy chain peptide (Life Technology Limited, peptide sequence RSLKLMATLFSTYASADR) emulsified in complete Freund's adjuvant (CFA), 7 days apart. A group of mice (controls) were injected only with CFA (Sigma, F5881). In all groups, the initial injection was also accompanied with an injection of pertussis toxin (Sigma, P7208) intraperitoneally. After the second myosin-CFA subcutaneous injection, one group of EAM mice were treated with a c-Met inhibitor (Sigma, PZ0147). Mice were sacrificed 28 days after the initial injection, the hearts removed and stained with H&E to score myocarditis severity by two blinded observers; myocarditis was graded from 1 to 4 (most severe). Cells from these mice were analyzed immediately after harvesting.

Assessment of cardiac function *in vivo*

Echocardiography was performed on mice to assess cardiac structure and function on day 0 and day 21 after immunization, using a Vevo-3100 imagining system (VisualSonics, Toronto, Ontario, Canada).

Mice were anaesthetized using 3% isoflurane together with 0.2L/min oxygen in an anesthesia chamber. Once sedated, mice were transferred to the echocardiography table, allowed to stabilize for at least 10 minutes and maintained using 2% isoflurane together with 0.4L/min oxygen via nosecone for the duration of the procedure. Mice limbs were then taped down onto the metal ECG leads on the platform. The platform was heated to 40°C, to ensure the body temperature of the animals was maintained throughout the procedure. Body temperature was continuously monitored with a rectal thermometer and the heart rate was monitored throughout the procedure from the ECG trace. Echocardiography gel, which was pre-warmed, then placed on the mice shaved chest to allow measurements to be taken using the scan head probe.

Images from two-dimensional brightness mode (B-mode) and one-dimensional motion mode (M-mode), were obtained.

Echocardiographic analyses were performed by two independent operators.

Hematoxylin and Eosin (H&E) staining

After removal, hearts were embedded in paraffin. Briefly, hearts were dehydrated with 95% ethanol for 0.5 h, twice, and then soaked in xylene for 1 h at 60 °C, followed by embedding in paraffin for 12 hours at room temperature. Paraffin-embedded tissue blocks were then cut into 7 µm-slices, dewaxed, mounted with neutral balsam. Slides were first soaked in Harris' hematoxylin solution for 6 h at a temperature of 60 °C and rinsed under a running tap until the water was colorless. Next, slides were incubated in 10% acetic acid and 85% ethanol for 3 minutes in water then soaked in saturated lithium carbonate solution for 12 h and then rinsed with tap water. Finally, staining was performed with eosin Y ethanol solution for 48 h. Tissue was imaged using Panoramic 250 High Throughput Scanner Microscope.

Masson's Trichrome staining

Paraffine-embedded hearts sections (4 µm) were deparaffinized and hydrated into xylol at 100% for 15 minutes (Sigma, cat 1330-20-7), then in an ethanol solution series (100%-95%-80%) for 2 minutes in each step, and finally in deionized water for 2 minutes. Samples were placed in a preheated Blouin's Solution (Sigma kit HT10132) at 56oC for 1 hour. After cooling down, slides were rinsed in running water until the water was colorless. Two drops of Working Weigert's Iron Hematoxylin Solution (Sigma kit HT1069) were added for 10 minutes before the slides were washed with deionized water, followed by a Biebrich Scarlet-Acid Fucshin (Sigma kit HT15) staining for 5 minutes and a further washing with deionized water. Anile Blue Solution (Sigma kit HT15) was added for 2 minutes followed by Phosphotungstic/Phospholybdic Acid solution (Sigma

kit HT15) for 15 minutes to allow the staining of all tissue components other than connective tissue fibers with Aniline Blue. Then Anile Blue Solution was added again for 3 minutes and then removed with 1% Acetic Acid (Sigma, 537020). Slides were dehydrated through two washes with 100% ethanol followed by xylene and finally mounted with aqueous mounting medium (Abcam, ab128982).

Histopathology

Evidence of myocarditis and fibrosis was evaluated by scanning 3x slides with 3x different transverse heart sections in Panoramic 250 High Throughput Scanner and hematoxylin/Eosin (H&E)-stained sections were categorized according to a 5-tier scoring system (experimental autoimmune myocarditis EAM score: grade 0, no inflammation; grade 1, mononuclear cell infiltration in up to 5% of the cardiac sections; grade 2, 6% to 10%; grade 3, 11% to 30%; grade 4, 31% to 50%; and grade 5, >50%. The score was performed by two independent operators, of whom one blinded.

Flow Cytometry (murine samples)

Cells were resuspended (10^7/ml) and incubated with fluorochrome-conjugated antibodies in 100 ul of flow cytometry buffer made of PBS containing 0.1% sodium azide (Sigma-Aldrich,S2002-25G) and 1% FBS at 4oC for 30 minutes. Following staining, cells were washed and resuspended with flow cytometry buffer and analyzed immediately. Alternatively, cells were fixed in fixation buffer (containing 1% Formaldehyde, Sigma-Aldrich,15,812-7) for 30 minutes at 4^{o}C, washed and stored in flow cytometry buffer at 4^{o}C.

For intracellular staining, cells were fixed and permeabilized for 30 minutes at 4oC using fixation/permeabilization working solution made by mixing 1 part of the fixation/permebilization concentrate (eBioscience, 00-5123) to 3 parts of the fixation/permebilization diluent (eBioscience,00-5223). Cells were then washed twice in 1X permeabilization buffer (eBioscience,00-8333) and stained with fluorochrome-conjugated antibodies in 1x permeabilization buffer for 30 minutes at 4^{o}C.

A final wash with 1x permeabilization buffer was performed and the cells were then centrifuged and resuspended in 200µl of flow cytometry buffer before fluorescence levels were measured using a BD LSRFortessa™ cell analyzer. Results were subsequently analyzed using the FlowJo software Version 10.

Cytokine measurement (mouse cells)

Spleens were harvested and homogenized through cell strainers, and erythrocyte removed with RBC lysis buffer (ThermoFisher, cat 00-4333-57). Cells were resuspended in 200µL of RPMI-1640 media (GIBCO, cat A10491-01). A cocktail containing Brefeldin A (10 µg/ml), PMA 10 ng/ml and Ionomycin 1µg/ml was added to the cells to induce cytokine production, while only RPMI-1640 media supplemented with a 10 µg/ml concentration of Brefeldin A (cat. 420601) was used as a control. The cells were left in the 5% CO2 incubator at 37°C for 5h, followed by surface and intracellular staining.

Antigen specificity in EAM

Two weeks after immunization, splenocytes ($2x10^7$) were labelled with CFSE (1 µg, Life Technology, C1157) and restimulated with 1 µM MHC peptide, along with 2 µg/ml of costimulatory α-CD28 (clone 37.51). Dilution of CFSE by $cMet^+$ and cMet- T-cells was assessed 7 days later by flow cytometry. To assess the cytokine production, splenocytes were stimulated as above for 6 hours. 10 µg/ml brefeldin A was added for the last 5 h. Cells were washed twice and stained with antibodies recognizing surface markers for 20 min at 4°C. Cells were permeabilized (Cytofix/Cytoperm Plus; BD) and stained with anti-cytokine antibodies for 20 min at room temperature prior to flow cytometric analysis.

Serum IL-4 ELISA

Mouse Enzyme-Linked Immunosorbent Assay (ELISA) IL-4 kit was purchased from StemCell 02038A. Assays were performed according to the manufacturer's instructions. Briefly, 96 wells plate has been pre-coated with Ms IL-4 antibody. 100µl Samples and 100µl standards were then added into pre-coated wells and bind to the immobilized (capture) antibody. The sandwich is formed by the addition of the second (detector) antibody, a substrate solution is added that reacts with the enzyme-antibody-target complex to produce measurable signal. OD readings at 450nm were converted to pg/ml using a standard curve and the appropriate dilution factor. Serum mouse samples were diluted 1:10 with Standard Diluent Buffer.

Flow Cytometry Analysis

Dedicated software was used to analyze the flow cytometry files (FlowJo version 10, FlowJo LLC, Oregon, USA). Gating for live cells was based on forward and side scatter profiles or exclusion with an amine-reactant dye that is non-permeant to live cells. FMO controls were used to precisely gate markers without distinct positive and negative populations. After the PBMC co-

culture assay the data was analyzed via automated proliferation analysis with the percentage of cells dividing from peak 0 compared.

Supplemental Tables S1-S5

Table S1 - Reagents and tools

Antibodies		
CCR4 PE-Cy7	Biolegend	Cat#359410
CCR4 BV421	Biolegend	Cat#359414
CCR7 BV605	Biolegend	Cat#353224
CD127 BV650	Biolegend	Cat#353126
CD25 AF700	Biolegend	Cat#356118
CD25 PE-Dazzle 594	Biolegend	Cat#356126
CD28 PE-Cy5	Biolegend	Cat#302910
CD4 PE	Biolegend	Cat#300508
CD4 APC-Cy7	Biolegend	Cat#300518
CD45RA PerCP-Cy5.5	Biolegend	Cat#304122
CD45RO BV785	Biolegend	Cat#304234
CD57 PE-Cy7	Biolegend	Cat#359624
CD69 BV510	Biolegend	Cat#310936
CD69 AF700	Biolegend	Cat#310922
CD8 Cy5	Southern Biotech	Cat#9536-15
CD8 PE-Dazzle 594	Biolegend	Cat#301032
CD95 BV510	Biolegend	Cat#305640
c-Met FITC	Thermofisher	Cat#11-8858-42
CX3CR1 APC-Cy7	Biolegend	Cat#341616
CXCR3 BV711	Biolegend	Cat#353732
FoxP3 PE-Dazzle 594	Biolegend	Cat#320126
FoxP3 PE	Thermofisher	Cat#12-4776-42
GARP PE	Biolegend	Cat#352504
GARP APC	Biolegend	Cat#352506
IFN-gamma APC	Biolegend	Cat#502512
IL-17A BV510	Biolegend	Cat#512330
IL-22 PE-Cy7	Biolegend	Cat#366708

IL-4 PE	Biolegend	Cat#500704
PD-1 BV421	Biolegend	Cat#329920
CD3	Origene	Cat#UM500048
c-Met	Thermofisher	Cat#ab51067
Cy5 goat anti-mouse	Thermofisher	Cat#A10524
FITC goat anti-rabbit	Thermofisher	Cat#F-2765
4,6 -diamidino-2-phenylindole	Thermofisher	Cat# D1306
IL 17 BV605	Biolegend	Cat#506927
IL 13 APCef780	Fisher Scientific	Cat#47-7133-80
IFNgamma APC	Fisher Scientific	Cat#17-7311-81
TNFalfa PECy7	Biolegend	Cat#506324
c-Met PE	Fisher Scientific	Cat#12-8854-82
CD8 FITC	Biolegend	Cat#100706
CD3 AF700	Biolegend	Cat#152316
CD4 eFluor 450	Fischer Scientific	Cat#48-0042-82
CD44 BV605	Biolegend	Cat#103047
CD69 PECy7	Fisher Scientific	Cat#25-0699-42
CD25 PECy5	Biolegend	Cat#102010
FOXP3 APC	Fisher Scientific	Cat#17-5773-82
anti-CD28	Invitrogen	Cat# 16-0281-86
CFSE	Life Technology	Cat#C1157
Tag-it-violet	Biolegend	Cat# 425101

Chemicals and Antigens

Xylene	Sigma	Cat#1330-20-7
Ethanol	Sigma	Cat#51976
Goat serum buffer	Sigma	Cat#G9023
Acetic Acid	Sigma	Cat#537020
Aqueous mounting medium	Abcam	Cat#ab128982
Cardiac myosin heavy chain peptide	Thermofisher	Cat#A4941-1

Complete Freund's adjuvant	Sigma	Cat#F5881
Pertussis toxin	Sigma	Cat#P7208
PHA665752	Sigma	Cat#PZ0147
RPMI 16400 medium	GIBCO	Cat#A10491
FBS 10%	Seralab	Cat#A20109
Sodium azide	Sigma	Cat#S2002
Formaldehyde	Sigma	Cat#15812-7
Tetanus Toxoid	Sigma	Cat#582231
Myosin light chain	Sigma	Cat#M4824
Myosin heavy chain	Sigma	Cat#M5074
Troponin T	Sigma	Cat#T0175
Troponin I	Sigma	Cat#T9924
Myoglobin	Sigma	Cat#M6036
Blouin's Solution	Sigma	Cat#HT10132
Working Weigert's Iron Hematoxylin Solution	Sigma	Cat#HT1069
Biebrich Scarlet-Acid Fucshin	Sigma	Cat#HT15
Anile Blue Solution	Sigma	Cat#HT15
Phosphotungstic/Phospholybdic Acid solution	Sigma	Cat#HT15
IL4 ELISA	Cell	Cat#0203814
IL13 ELISA	Abcam	Cat#KMC2221
Mouse Strain		
Balb/cAnN	Charles River Laboratories UK Ltd	Cat# 000654
NOD	Jackson Laboratory	Cat#001976
Software and Algorithms		
ImageJwin64 V 1.52p	ImageJ	https://imagej.nih.go
Vevo-3100 imagining system	Vevo	https://www.visualsonics.com/imaging-systems/vevo-3100
Graph Pad 8.3.0	GraphPad	https://www.graphpad.com
FlowJo V10	FlowJo	https://www.flowjo.com

Table S2: Baseline characteristics of the subject groups.

	AM (n=34)	iDCM (n=31)	STEMI (n=15)	HC (n=20)	SS (n=7)	fHMD (n=14)	IHF (n=8)	CS (n=11)
Age at enrolment	35 (13)	59 (15)	54 (13)	31 (6)	57 (8)	44 (14)	67 (10)	71 (7)
Male (%)	25 (74)	20 (65)	12 (80)	12 (60)	3 (17)	6 (43)	13 (87)	8 (73)
Ethnicity (%)								
White	15 (44)	15 (48)	6 (40)	14 (70)	12 (67)	13 (93)	12 (80)	10 (91)
Asian	1 (3)	1 (3)	3 (20)	6 (30)	3 (17)	1 (7)	3 (20)	1 (9)
Black	5 (15)	3 (10)	1 (7)	0	2 (11)	0	0	0
Other	3 (9)	12 (39)	4 (27)	0	0	0	0	0
Not stated	10 (30)	0	1 (7)	0	1 (6)	0	0	0
Days from admission to enrolment	6 (12)		2 (2)					
Admission to CMR	6 (12)							
Peak Troponin T, ng/L	1040 (999)		1660 (2704)					
AM presentation type (%)								
ACS	32 (94)							
CCF	1 (3)							
Arrhythmic	1 (3)							
Evidence for absence of coronary disease in acute myocarditis								
Angiogram (%)	23 (68)							
Low clinical suspicion (%)	11 (32)							

AM: acute myocarditis. iDCM: idiopathic dilated cardiomyopathy. STEMI: ST elevation myocardial infarction. HC: healthy control. SS: Sjögren's syndrome. fHMD: familial heart muscle disease. IHF: ischemic heart failure. CS: patient undergoing elective cardiac surgery. CMR: cardiac magnetic resonance imaging. ACS: acute coronary syndrome. CCF: congestive cardiac failure. Data are presented as mean (SD) or total number (%)

Table S3: Demographics and baseline characteristics of patients with AM (autopsy for sudden death) and iDCM (autopsy for sudden death or ventricular assistance device/cardiac transplantation).

Age at enrolment	32 (1-48)	53 (36-66)
Male (%)	4 (80)	3 (60)
Ethnicity (%)		
White	5 (100)	5 (100)
Days from admission to enrolment	1 day	months
Peak Troponin T, ng/L	N.A.	N.A.
AM presentation type (%)	N.A.	N.A.
Ventricular arrhythmias/Sudden death (%)	5 (100)	2 (40%)
CCF (%)	0	3 (60%)
EF (%)	N.A.	21 (19-23)
Angiogram (%)	N.A.	0
At gross and histological exam	0	0

Table S4: Genetic heart muscle disease patients' pathogenic genetic mutations

	Gene	Protein change	Pathogenicity
1	Desmoplakin (DSP)	p.Arg1392Gln	Likely pathogenic
2	Desmoplakin (DSP)	p.Trp1342*	Pathogenic
3	Desmoplakin (DSP)	p.Asn274Glufs*15	Pathogenic
4	Desmoplakin (DSP)	p.Lys1887fs*	Pathogenic
5	Desmoplakin (DSP)	p.Lys2523Glnfs*37	Pathogenic
6	Desmoplakin (DSP)	p.Cys2656Trpfs*24	Very likely pathogenic
7	Filamin-C (FLNC)	p.Arg482*	Very likely pathogenic
8	Lamin A/C (LMNA)	p.Arg25Cys	Pathogenic
9	Plakophilin-2 (PKP-2)	p.His733Alafs*8	Pathogenic
10	RNA binding motif protein 20 (RBM20)	p.Arg636Cys	Pathogenic
11	Titin (TTN)	p.Arg11944*	Very likely pathogenic
12	Titin (TTN)	p.Cys19065Valfs*44	Very likely pathogenic
13	Titin (TTN)	p.Arg6767*	Very likely pathogenic
14	Tropomyosin alpha-1 (TPM1)	p.Asp84Asn	Very likely pathogenic

Table S5: Differentially expressed Gene pathways in $CD4^+$ and $CD8^+$ $cMet^+$ T-cells

$CD4^+cMet^+$ T-cells

Pathway Name	Gene Found	Gene Pathway	Percentage	P value	enriched genes
Olfactory transduction	14	388	0.04	4.09115E-07	OR12D2, OR14J1, OR1I1, OR1L3, OR1S1, OR4A15, OR4D10, OR51D1, OR5F1, OR5M1, OR5M8, OR6T1, OR7A17, OR7C1
Hematopoietic cell lineage	3	88	0.03	0.0074103	CD22, CD24, FCGR1A
Regulation of actin cytoskeleton	4	214	0.02	0.037111487	ABI2, F2, NCKAP1, PAK5

$CD8^+cMet^+$ T-cells

Pathway Name	Gene Found	Gene Pathway	Percentage	P value	Enriched genes
Pancreatic secretion	3	101	0.03	0.006672165	CA2, CPB2, PLA2G2A
Olfactory transduction	7	388	0.02	0.005678544	OR12D3, OR2T2, OR4P4, OR5P2, OR6C6, OR8D2, OR8G2P
Metabolic pathways	4	1131	0	0.871898063	CDA, PGK2, PLA2G2A, XYLB

Supplemental Figures

Figure S1:

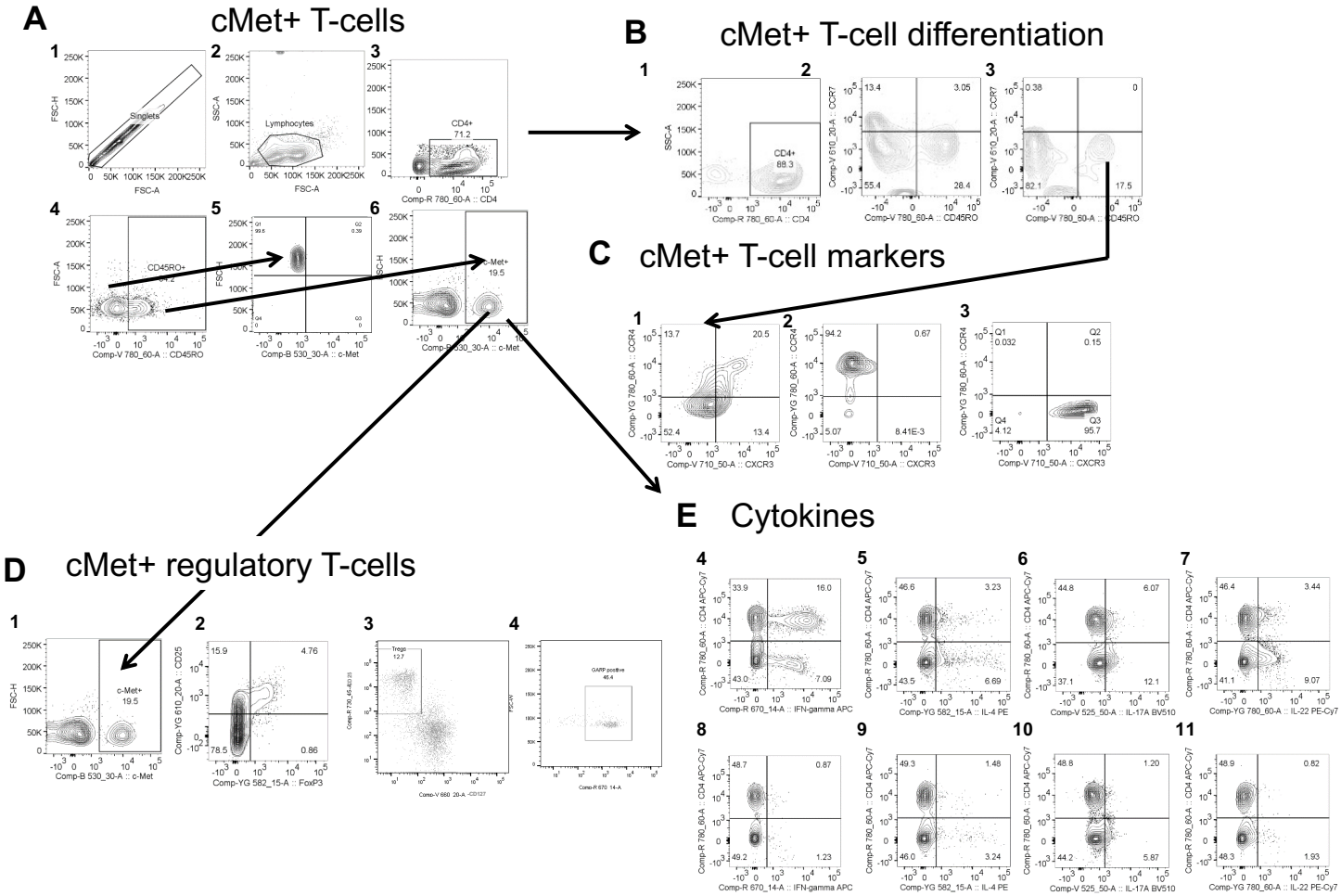

Gating strategies for flow cytometric analysis of human T-cells.

A, Exemplar flow cytometry gating strategy to define Singlets (1), Lymphocytes (2), $CD4^+$ T-cells (3), $CD45RO^+$ memory T-cells (4) and the proportion of $CD4^+$ $CD45RO^-$ (naïve, 5) and $CD4^+$ $CD45RO^+$ (memory, 6) T-cells that are c-Met^+ in an acute myocarditis patient. The same approach was used following gating on $CD8^+$ T-cells.

B, gating strategy for the identification of differentiation stage of cMet^+ T-cells.

C, gating strategy for the identification of cell marker expression by cMet^+ T-cells (example depicts CXCR3 and CCR4, can be applied to CD69, CD95 etc.)

D, gating strategy for the identification of regulatory cMet^+ T-cells.

E, gating strategy for the identification of cytokine production by $CD4^+$ T-cells.

The sequence of gates is indicated by progressive numbering.

Figure S2:

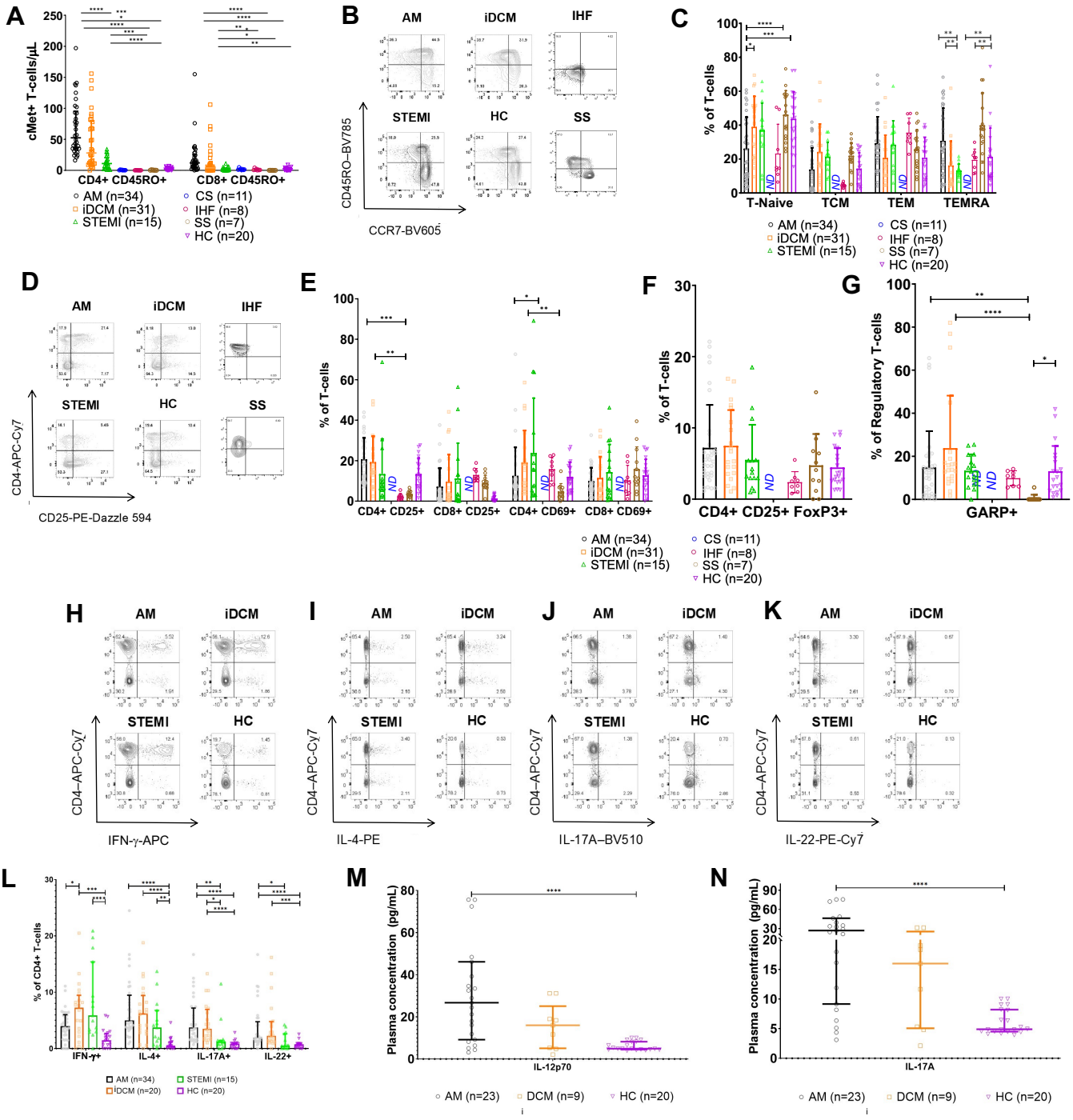

Characterization of the immune response in patients and controls.

A, Absolute c-Met^{+} T-cell count (cells/uL) in CD4^{+} and CD8^{+} CD45RO^{+} populations across different subject cohorts. AM, acute myocarditis; iDCM, idiopathic dilated cardiomyopathy; STEMI, ST-segment elevation myocardial infarction; CS, cardiac surgery; IHF, ischemic heart failure; SS, Sjögren' s Syndrome; HC, healthy controls).

B, Representative flow cytometry plots of peripheral blood $CD4^+$ T-cells with CD45RO on the y-axes and CCR7 on the x-axes as example plots for patients in each of the main patient groups

C, Summary data for the patient groups (the number of subjects in each group are shown in parentheses below the chart). T naïve: $CD45RO^-$ $CCR7^+$, TCM: $CD45RO^+$ $CCR7^+$, TEM: $CD45RO^+$ $CCR7^-$, TEMRA: $CD45RO^-$ $CCR7^-$).

Statistical analysis was performed using a one-way ANOVA.

D, Representative flow cytometry dot-plots of peripheral blood $CD4^+$ $CD25^+$ T-cells in the four main patient groups.

E, Summary data for the expression of CD25 and CD69 for both $CD4^+$ and $CD8^+$ T-cells in the patient groups. Statistical analysis was performed by one-way ANOVA.

F-G, Peripheral blood $CD4^+$ T-cells from the groups indicated were analyzed by flow cytometry for the expression of FoxP3 and high levels of CD25 and, within this population T-cells expressing the suppression marker glycoprotein A repetitions predominant (GARP). The number of patients in each group is also indicated below the Y axis. Data were compared among the patient groups and between different patient groups. Statistical analysis was performed using a two-way ANOVA test with no significant difference in the proportion of T-regs although significant differences in the proportion of T-regs that were GARP positive (post-hoc Tukey's multiple comparison test between DCM and HC).

H-K, Representative dot plots depicting intracellular cytokine staining of peripheral blood $CD4^+$ T-cells from the indicated groups.

L, Summary data of the production of the indicated cytokines by each group. The patient groups and the number of patients in each group is shown below the x-axis. Statistical analysis was performed with Kruskal-Wallis tests ($p<0.0001$ for each intracellular cytokine) with post-hoc Dunn's multiple comparisons tests.

M-N, Plasma multiplex ELISA was performed to measure concentrations of cytokines and the chemokine CXCL10 in the indicated groups. Kruskal-Wallis tests were significant for interleukin (IL) 12p70 (panel M) and IL-17A (panel N). Post-hoc Dunn's comparisons tests were significant for comparison of IL-12p70 between AM and HC and of IL-17A between AM and HC.

The patient groups and the number of patients in each group are shown below the x-axis.

P values are highlighted as: ****$p<0.0001$, ***$p<0.001$, **$p<0.005$, *$p<0.05$

A-K: data shown as mean±SD

L-N: Data represented as median and interquartile range.

Comment. By comparing the whole memory T-cell populations we observed a reduction in the proportion of circulating naïve T-cells in AM patients (**B-C**), as well as an increase in memory $CD4^+$ T-cells expressing the activation markers CD25 and CD69 (**D-E**). Terminally differentiated CCR7- CD45RO- $CD8^+/CD4^+$ (TEMRA) T-cells [25] were increased in all the patients samples compared to healthy controls (**C**). No differences were observed in $CD4^+$ CD25high $FoxP3^+$ regulatory T-cells (Treg) and of Treg cells expressing glycoprotein A repetitions predominant (GARP, **F-G**) a marker of Treg activation [26], except a significantly low expression of this molecule by SS Tregs.

Compared to HC, the proportion of all $CD4^+$ T-cells (i.e., $cMet^{+/-}$) producing IL-4 was significantly increased in AM, iDCM and STEMI patients (**H-L**), and IL-17A and IL-22 production was approximately double in both AM and iDCM patients compared with HC and STEMI. In addition, IFN-γ-producing T-cells were increased in AM patients, iDCM patients and STEMI patients compared to HC (**H-L**). Finally, we detected a significant increase in plasma IL-12p70 and IL-17A in patients with AM compared to HC (**M-N**, respectively), while there was no significant difference in the plasma concentrations of HGF, CXCL10, IFN-γ, IL-4, IL-10, TGF-β and TNF-α between the groups (not shown).

Figure S3:

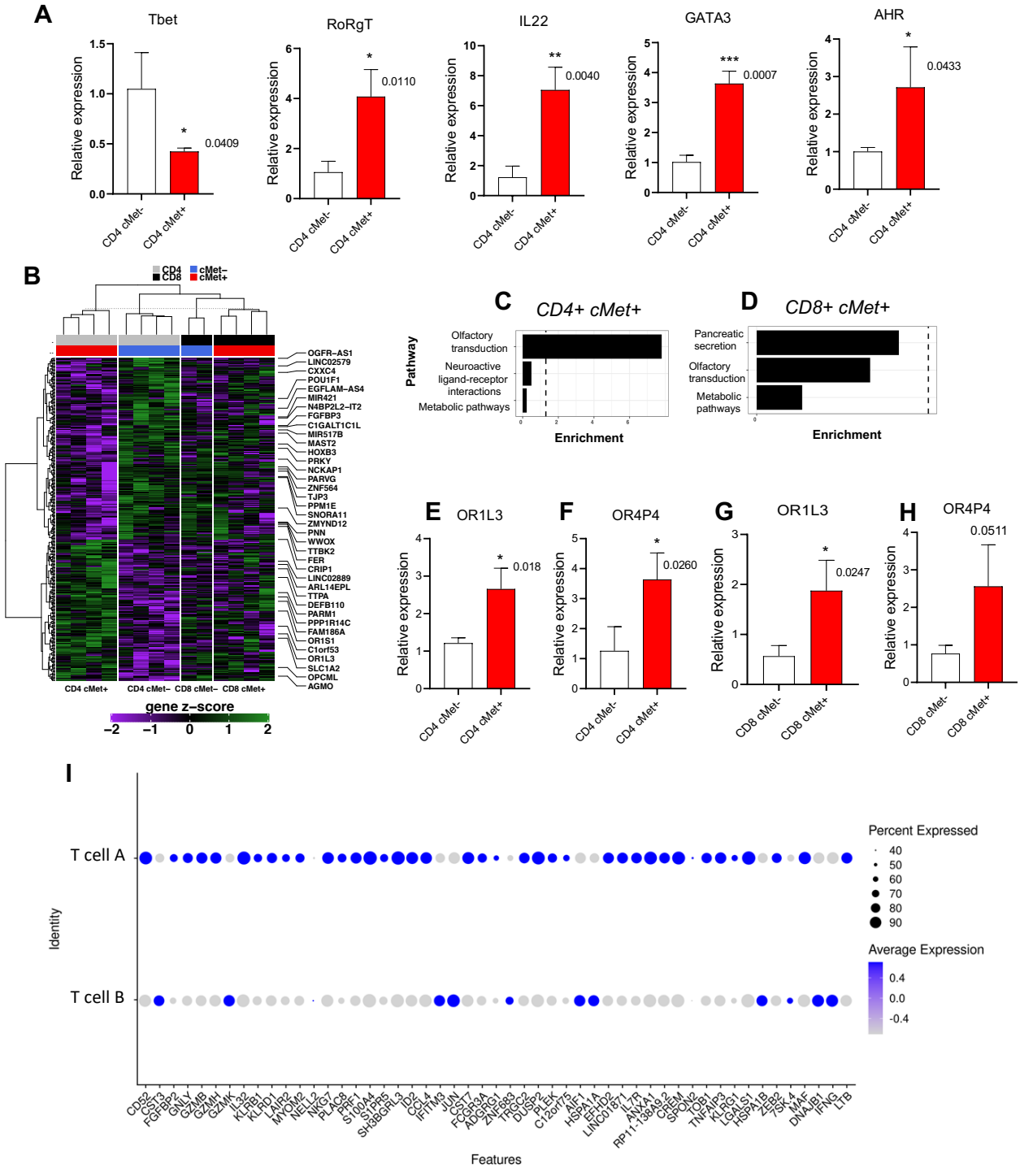

RNA expression profile of cMet⁺ T-cells.

To gain further insight on the characteristics of cMet T-cells, $CD4^+$ and $CD8^+$ T-cells were purified by negative selection from PBMCs containing at least 7% cMet T-cells and controls <0.5% $cMet^+$ T-cells (n=8). T-cells were subsequently stimulated in vitro with anti-CD3/CD28

antibodies. Cells were harvested 72 hours later, and mRNA extracted for analysis. on. As in human T-cell, staining with the anti-cMet antibody requires fixing and permeabilizing the T-cells, it was not possible to isolate RNA in sufficient amounts from purified $cMet^+$ T-cells. **A**, Expression of cytokine-regulating genes by cMet-enriched ($cMet^+$) and control ($cMet^-$) $CD8^+$ T-cells.

B, Heatmap of RNA-Seq expression z-scores computed for genes that are differentially expressed between cMet-enriched ($cMet^+$) and control ($cMet^-$) $CD4^+$ and $CD8^+$ T-cell populations using Affymetrics arrays. **C-D**, Gene ontology over-representation analysis of genes significantly increased in CD4 and $CD8^+$ $cMet^+$ T-cells. Enrichment score is –Log10 adjusted p-value (KEGG) or –Log10 Kolmogorov-Smirnov p-value (GO). (EF) Validation by RTpcr of some of the genes differentially expressed by cMet-enriched ($cMet^+$) and control ($cMet^-$) T-cells.

E-F, Validation by RT-PCR of some of the genes differentially expressed by cMet-enriched ($cMet^+$) and control ($cMet^-$) in purified $CD3^+$ T-cells from HC (n=3) or DCM patients (n=3). Data are shown as gene expression relative to the housekeeping gene GADPH.

P values are highlighted as: ***p<0.001, **p<0.005 and *p<0.05. Comparison by t-test.

Comment: OR1L3 (Olfactory Receptor Family 1 Subfamily L Member 3) and (Olfactory Receptor Family 4 Subfamily P Member 3) encode for olfactory receptor proteins. Olfactory receptor (OR) proteins are members of a large family of G-protein-coupled receptors (GPCR) sharing a 7-transmembrane domain structure with many neurotransmitter and hormone receptors and are responsible for the recognition and G protein-mediated transduction of odorant signals. [28] ORs are known to be expressed by olfactory sensory neurons; in addition, their expression has been described all other human tissues tested to date, in circulating immune cells. Except from olfactory sensory neurons, their functional roles remain largely unknown. They have been shown to be involved in the modulation of cell-cell interaction, migration, proliferation, apoptosis, and exocytosis. [28]

I, Dot plot of differentially expressed genes T cell cluster A mostly resembling the cMet+ T cell subset) and T cell cluster B (the rest of the T cell populations). scRNA data was accessed from GEO GSE145154 and re-analyzed as previously described. [30]

Figure S4:

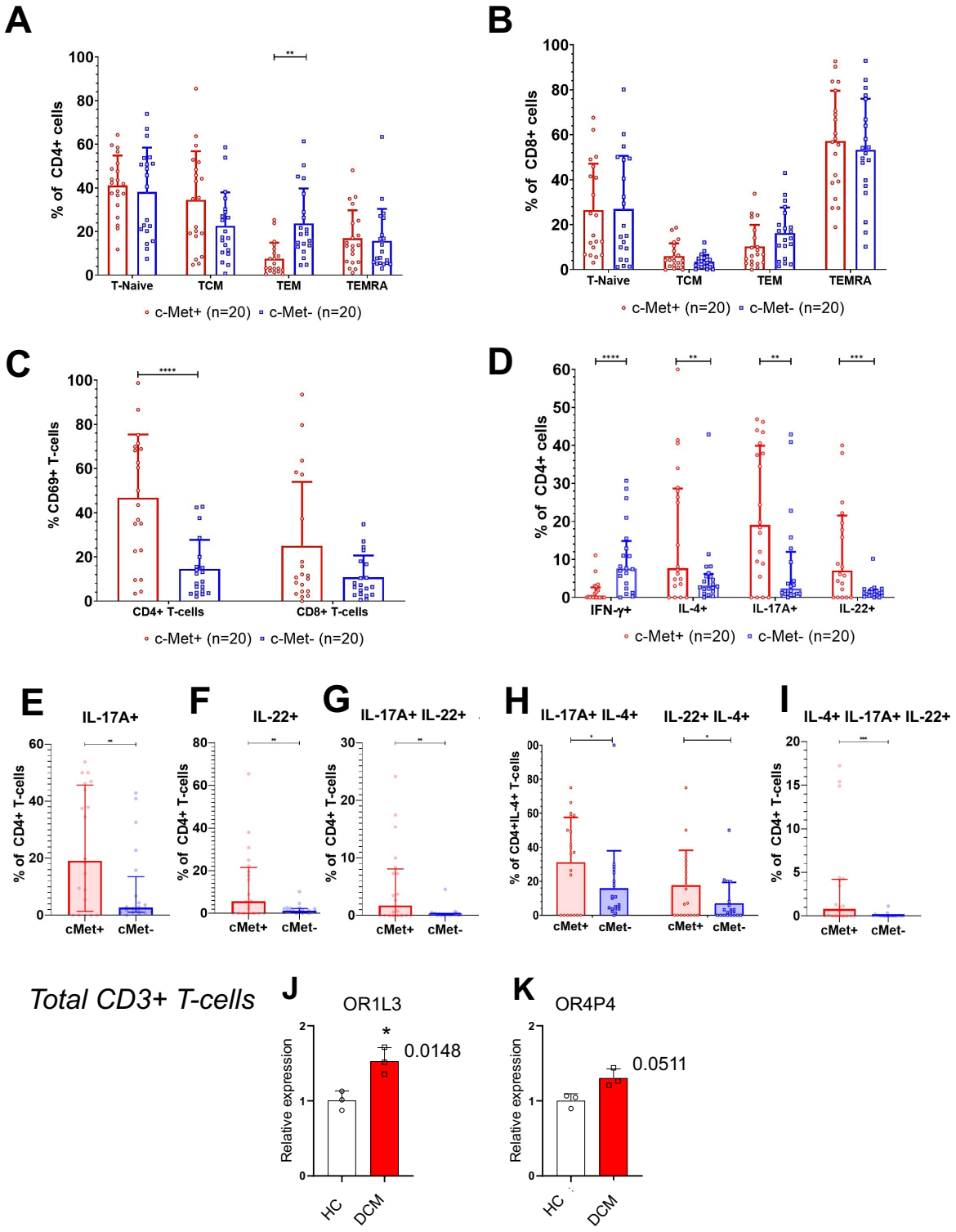

Phenotypic and functional comparison of cMet^{+} and cMet- T-cells in idiopathic dilated cardiomyopathy.

A-B, The proportion of cMet$^+$ and cMet- naïve, central memory (TCM), effector memory (TEM) or terminally differentiated effector T-cells (TEMRA) was determined by flow cytometric analysis of both CD4$^+$ and CD8$^+$ T-cell subsets from idiopathic dilated cardiomyopathy (iDCM) patients.

C, The proportion of cMet$^+$ and cMet$^-$ CD69-expressing CD4$^+$ and CD8$^+$ T-cells was determined by flow cytometry.

D, The production of the indicated cytokines by peripheral blood cMet$^+$ and cMet- CD4$^+$ T-cells from iDCM patients was assessed by flow cytometry. The number of patients in each group is shown in parentheses below the x-axis with the red dots representing c-Met positive cells and the blue dots representing c-Met negative cells. Statistical analysis was performed via Wilcoxon signed rank test with significant results for IFN-γ, IL-4, IL-17A and IL-22.

E-I, Analysis of multiple cytokine-producing cMet$^+$ and c-Met$^-$ memory T-cells. Panel **E** (IL-17$^+$); **F** (IL-22$^+$); **G** (IL17$^+$ and IL22$^+$); **H** (IL-4$^+$/IL17$^+$ and IL4$^+$/IL22$^+$); **I** (IL-4$^+$IL-22$^+$IL-17A$^+$). Statistical analysis was performed using repeated measures two-way ANOVA.

J-K, Validation by RT-PCR of some of the genes differentially expressed by cMet-enriched (cMet$^+$) and control (cMet-) in purified CD3$^+$ T-cells from HC (n=3) or DCM patients (n=3). Student's paired t-test.

P values are highlighted as: **** p<0.0001, *** p<0.0005, **p<0.01 and p*<0.05. Data are presented as median ± interquartile range

Comment: Like in AM, circulating CD4$^+$cMet$^+$ T-cells in iDCM patients displayed decreased proportions of memory T-cells with an effector phenotype, but no differences in naïve, central memory and TEMRA cMet$^+$ T-cells (**A-B**), as well as a significantly increased proportion of memory cMet$^+$ T-cells that were CD69$^+$ when compared to the cMet$^-$ subset (**C**).

Cytokine profiles of CD4$^+$cMet$^+$ memory T-cells in AM and iDCM patients were also similar, with greater proportions of CD4$^+$cMet$^+$ memory T-cells from iDCM patients producing IL-4, IL-17A and IL-22 (**D**). Like in AM, we detected a significantly increased population of IFN-γ-producing cMet$^-$ memory CD4$^+$ T-cells. Further analysis of multiple cytokine producer cMet$^+$ T-cells showed, like in AM, a significant increase in single positive IL-17A$^+$cMet$^+$ T-cells compared to cMet$^-$ cells (**E**). Likewise, single positive IL-22$^+$cMet$^+$ T-cells were increased compared to cMet- T-cells (**F**). IL-17$^+$IL-22$^+$ co-producing Th-cells were also increased in the circulating cMet$^+$ compared to cMet$^-$ memory Th-cell populations in iDCM (**G**). cMet$^+$ T-cells from iDCM were also significantly enriched in IL-4$^+$IL-17-A$^+$ co-producing T-cells. Interestingly, unlike in AM the IL-4$^+$IL-22$^+$ co-producing Th-cell subset was also significantly more abundant in the cMet$^+$ T-cell population. Finally, there was a significant increase in 'triple positive' IL-4$^+$IL-22$^+$IL-17A$^+$ T-cells within the cMet$^+$ T-cells (**I**).

Figure S5.

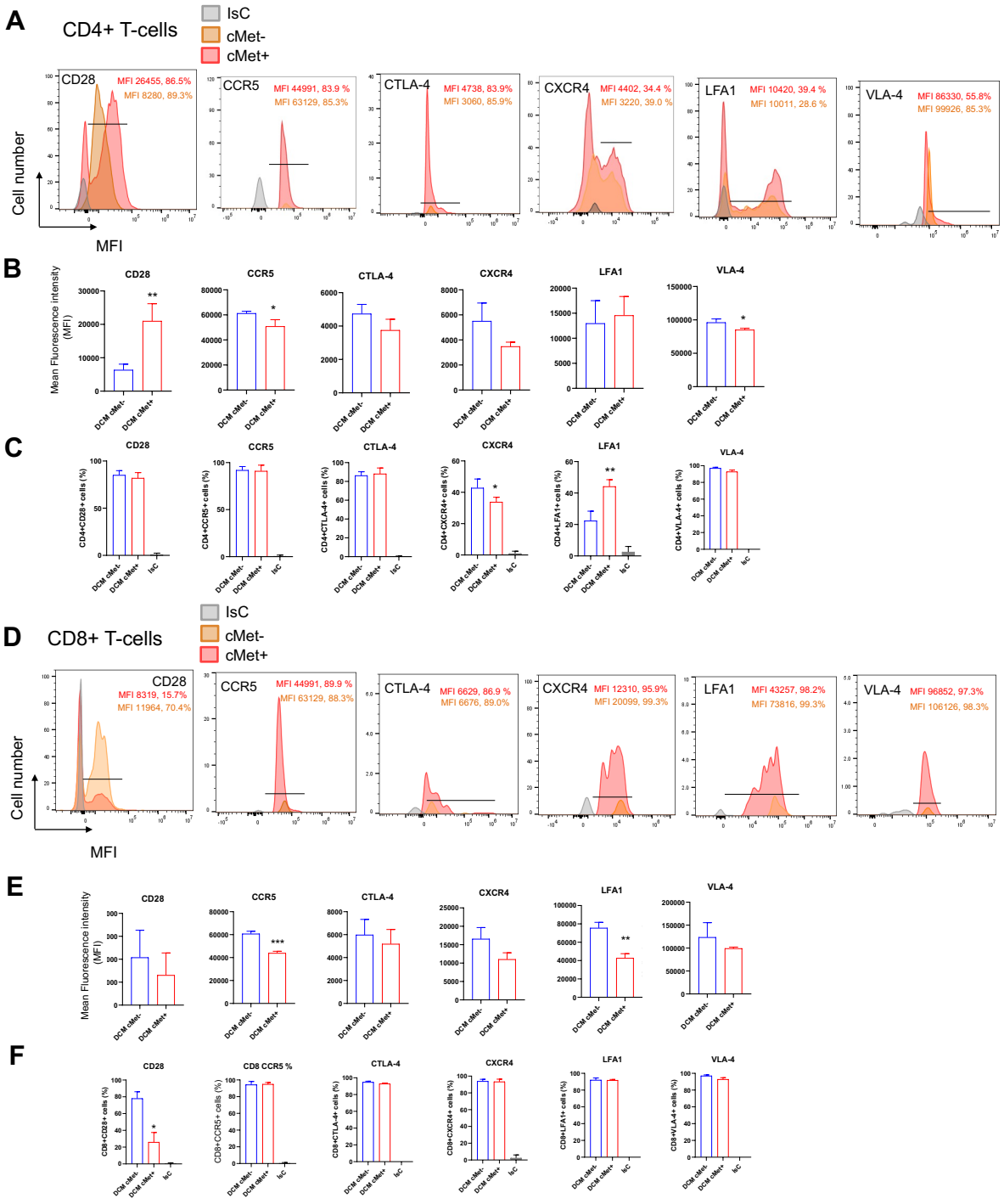

Phenotypic and functional characterization of cMet$^+$ T-cells in iDCM

Further characterization of cMet$^+$ T-cells in patients with iDCM was carried out by flow cytometry. **A**, representative histograms. The mean MFI and % ± SD of CD4$^+$ T-cells expressing the indicated molecules are shown in panels **B** and **C**, respectively (n=3). **D**, representative histograms. The mean MFI and % ± SD of CD8$^+$ T-cells expressing the

indicated molecules are shown in panels **E** and **F**, respectively (n=3). t-test. P values are highlighted as: *p<0.05, **p<0.01, ***p<0.005.

Figure S6.

A

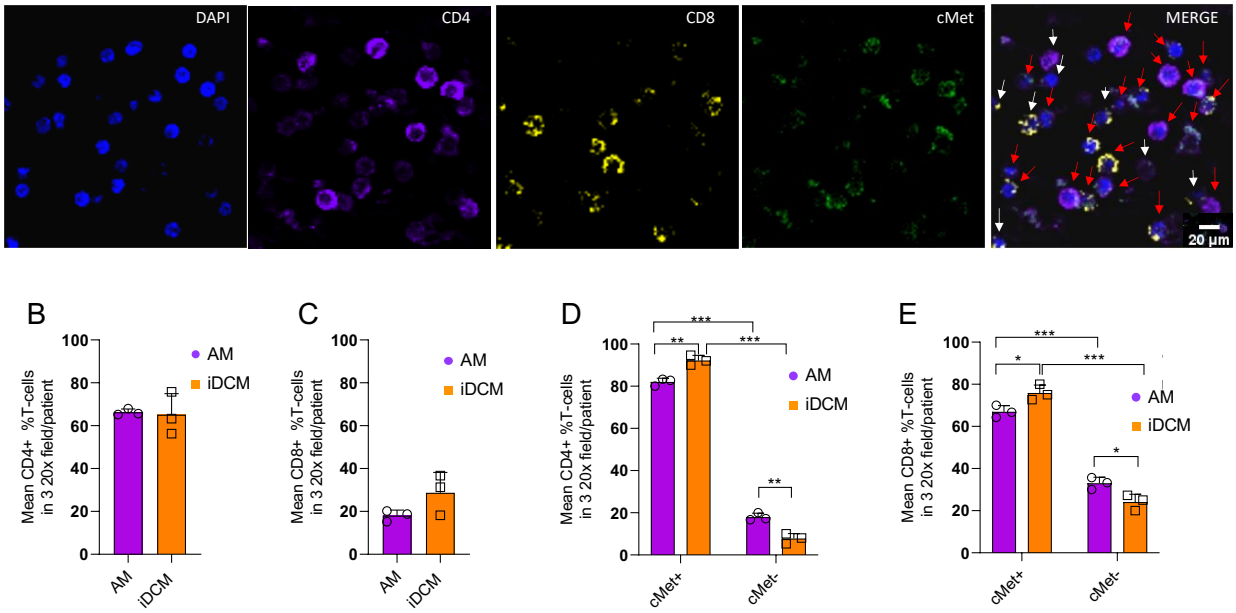

Percentage of CD4+ cMet+ and CD8+ cMet+ T-cells in AM and iDCM.

A, Representative confocal images of $CD4^+$ (magenta), CD8+ (yellow), $cMet^+$ (green) cells in a paraffin-embedded postmortem iDCM sample, white arrows indicate cMet- cells, red arrows cMet+. Scale bar: 20 μm. The column graph shows the mean percentage of CD4+ and CD8+ cells in three 20x field from each of 3 postmortem AM and iDCM samples (**B** and **C**, respectively) and the percentage of $cMet^+$ and cMet- T-cells within the $CD4^+$ and $CD8^+$ populations (**D** and **E**, respectively), ± SEM. Two-way ANOVA was used for comparing AM vs iDCM, paired Student t-Test for comparing cMet+ vs cMet- T-cells. in each population.
P values are highlighted as: *p<0.05, **p<0.01, ***p<0.005, and data are represented as median ± interquartile range.

Figure S7.

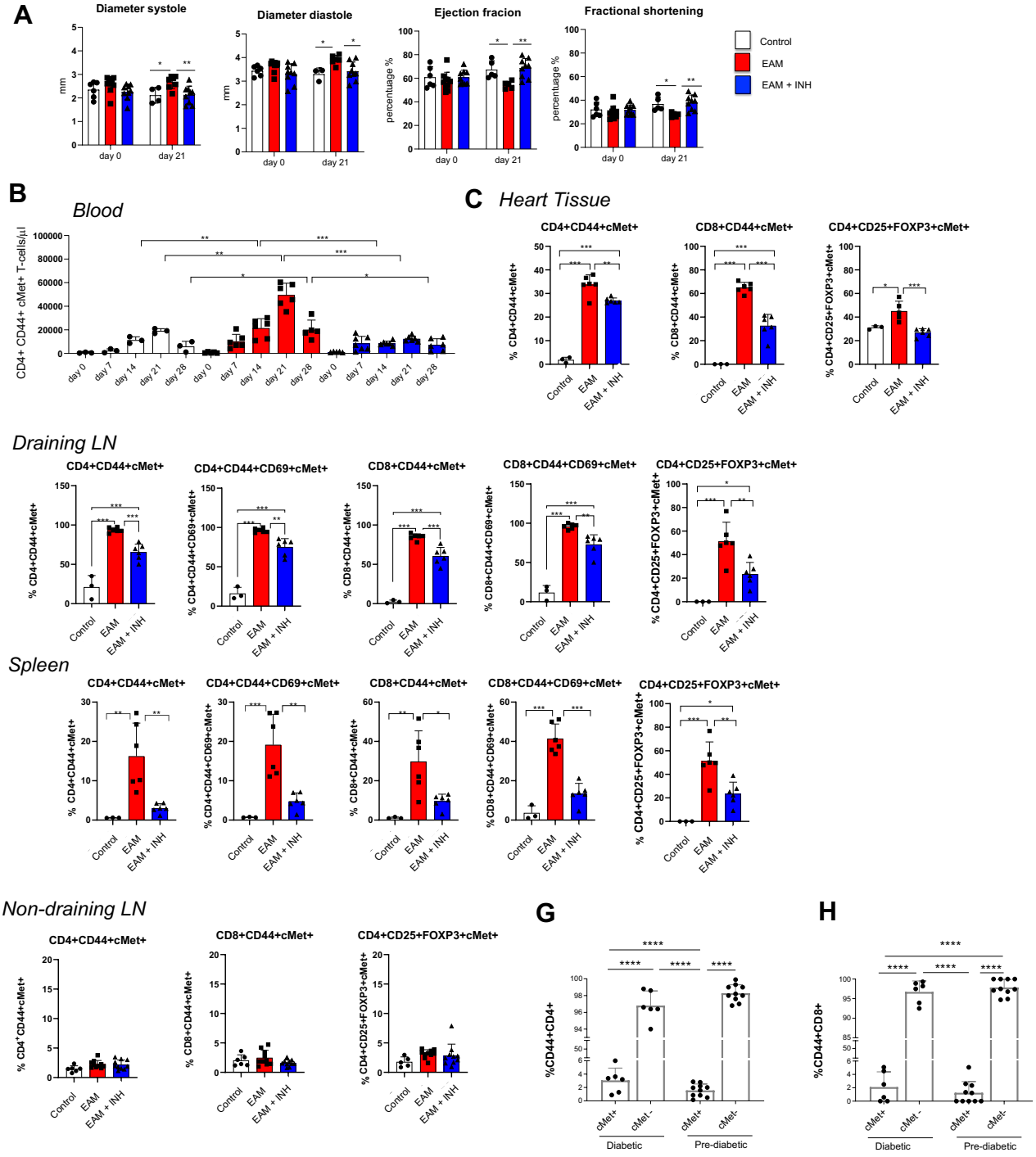

Phenotypic and functional characterization of cMet$^+$ T-cells in EAM

Balb/cAnN male mice were immunized with Murine cardiac myosin Myosin Heavy Chain (MHCα) peptide as described in Materials and Methods. As a control mice received adjuvant alone. A group of mice was treated with PHA665752 (500µg/ml) for 10 days after the second

immunization. Mice were sacrificed 28 days after immunization and their phenotype and function was investigated by flow cytometry.

A, Tail vein blood was sampled on the indicated time points. Absolute numbers of $CD44^{high}$, $CD4^{+}cMet^{+}$ T-cells was determined by flow cytometry. Statistical analysis was performed with two-way repeated measures ANOVA.

B, Functional cardiac parameters were measured by echocardiogram 23 days after immunization using two-way repeated measures ANOVA.

C-F, Expression of the indicated markers in the Heart tissue (B), Draining LN (C) Spleen (D) and non-draining LN (E) were analyzed in the different experimental groups. Statistical analysis was performed using by one-way ANOVA.

G-H, The presence of $cMet^{+}$ $CD4^{+}$ (F) and $CD8^{+}$ (G) T-cells was assessed in the blood of pre-diabetic (glucose levels higher than 150mg/dl) and diabetic (glucose levels higher than 250mg/dl) NOD mice by flow cytometry. Analysis by two-way ANOVA.

P values are highlighted as: *p<0.05, **p<0.01, ***p<0.001 and ****p<0.0001. Data are presented as median ± interquartile range

Figure S8:

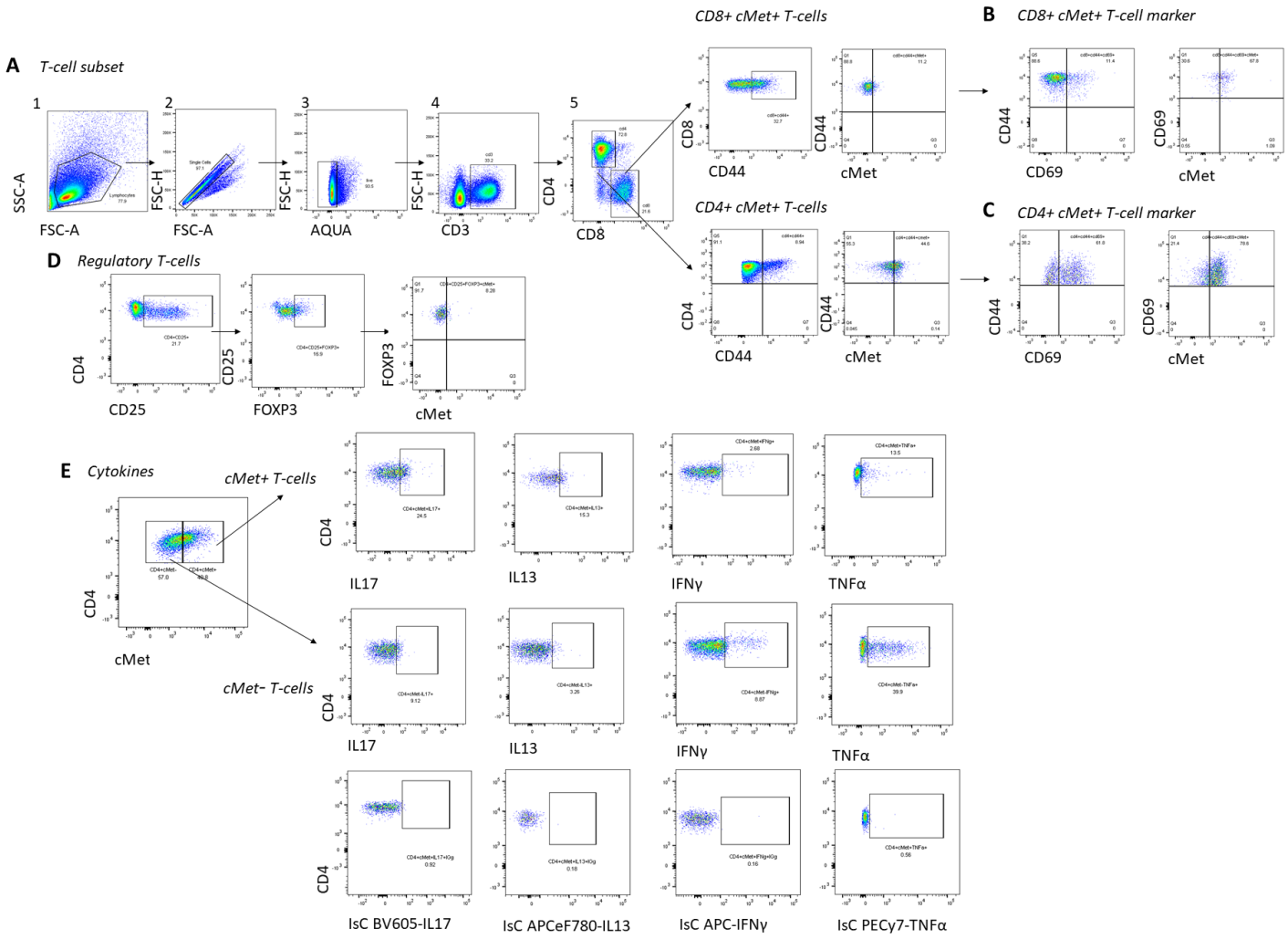

Gating strategy for the identification and characterization of cMet^{+} cT-cells in experimental autoimmune myocarditis.

A, Exemplar flow cytometry gating strategy to define Lymphocytes (1), Singlets (2), Live cells (3) CD3^{+} T-cells (4), CD4^{+}/CD8^{+} T-cells (5), CD44 high (6) and the proportion of CD4^{+} CD44^{high} T-cells that are c-Met^{+} (7) in EAM.

B-C, gating strategy for the identification of the expression of the indicated and other markers by cMet^{+} T-cells.

D, gating strategy for the identification of Tregs

E, gating strategy for the identification of intracellular cytokine production by cMet^{+} T-cell subsets including isotype control (IsC) for reference.

The gating sequence is indicated by progressive numbering.

Figure S9.

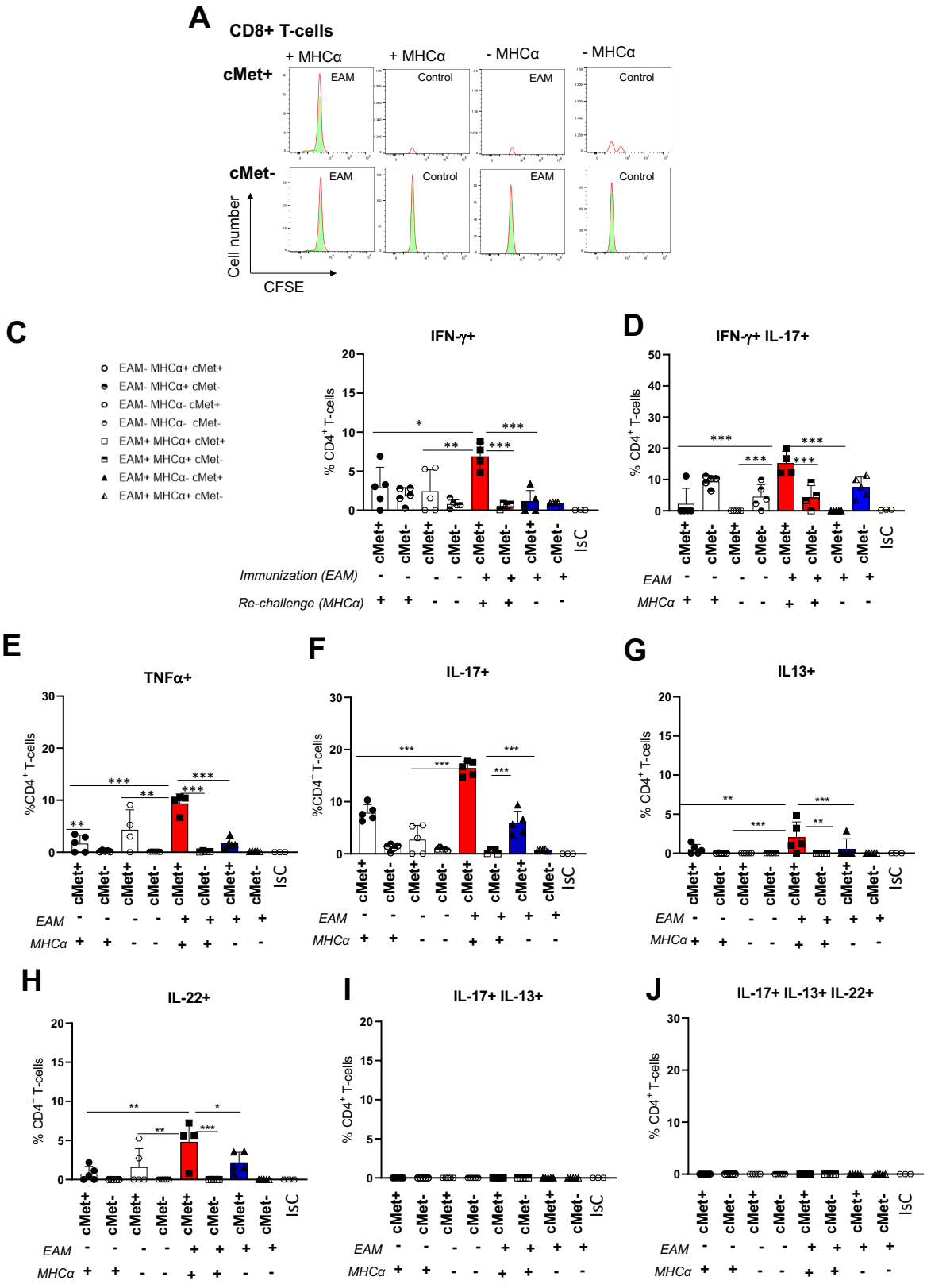
A
CD8+ T-cells
+ MHCα
+ MHCα
- MHCα
- MHCα
cMet+
cMet-
EAM
Control
Cell number
CFSE
C
EAM- MHCα+ cMet+
EAM- MHCα+ cMet-
EAM- MHCα- cMet+
EAM- MHCα- cMet-
EAM+ MHCα+ cMet+
EAM+ MHCα+ cMet-
EAM+ MHCα- cMet+
EAM+ MHCα+ cMet-
IFN-γ+
% CD4+ T-cells
Immunization (EAM)
Re-challenge (MHCα)
D
IFN-γ+ IL-17+
EAM
MHCα
E
TNFα+
%CD4+ T-cells
F
IL-17+
G
IL13+
H
IL-22+
I
IL-17+ IL-13+
J
IL-17+ IL-13+ IL-22+
cMet+
cMet-
IsC

Characteristics of cMet$^+$ T-cells in EAM.

Balb/cAnN male mice were immunized with Murine cardiac Myosin Heavy Chain (MHCα) peptide (RSLKLMATLFSTYASADR) as described in Materials and Methods.

Fourteen days after the second immunization, mice were sacrificed and CD8$^+$ T-cells from heart-draining LNs were labeled with CFSE and re-stimulated in vitro with autologous splenocytes, stimulatory anti-CD28 antibody and MHCα peptide. Controls included mice treated with adjuvant alone. Cells were harvested and analyzed 7 days later. Representative histograms are showing proliferation by cMet$^+$ and cMet$^-$ CD8$^+$ T-cells are shown in panel **B** (n=5).

C-J, fourteen days after the second immunization, mice were sacrificed and CD4$^+$ T-cells from the spleen were re-stimulated in vitro with autologous splenocytes, stimulatory anti-CD28 antibody and MHCα peptide. Production of the indicated cytokines by cMet$^+$ and cMet$^-$ T-cells was measured 6 hours after re-stimulation by intracellular staining. Data are shown as mean percentage of cytokine-expressing CD4$^+$ T-cells.

Statistical analysis was performed with a single mixed-effects ANOVA test, to account for the fact that some samples are paired and correlated.

P values are highlighted as: *p<0.05, **p<0.01 and ***p<0.0005. Data are presented as median ± interquartile range.